Original Article

Hyperglycemia-induced increasing of *RELB*/circ_0008590 in NF-κB pathway is repressed by miR-1243 in human retinal microvascular endothelial cells

Jun Shao[1#]^, Jiping Cai[1#], Yong Yao[1], Hui Zhu[2]

[1]Department of Ophthalmology, The Affiliated Wuxi People's Hospital of Nanjing Medical University, Wuxi, China; [2]State Key Laboratory of Reproductive Medicine, Department of Histology and Embryology, Nanjing Medical University, Nanjing, China

Contributions: (I) Conception and design: J Shao, J Cai; (II) Administrative support: Y Yao, H Zhu; (III) Provision of study materials or patients: J Shao, J Cai, Y Yao; (IV) Collection and assembly of data: J Shao, J Cai; (V) Data analysis and interpretation: J Shao, J Cai; (VI) Manuscript writing: All authors; (VII) Final approval of manuscript: All authors.

[#]These authors contributed equally to this work.

Correspondence to: Yong Yao. Department of Ophthalmology, Wuxi People's Hospital Affiliated to Nanjing Medical University, 299 Qingyang Road, Wuxi 214023, China. Email: yaoyongchina@outlook.com; Hui Zhu. State Key Laboratory of Reproductive Medicine, Department of Histology and Embryology, Nanjing Medical University, Nanjing 211166, China. Email: njzhuhui@njmu.edu.cn.

Background: To investigate the abnormal expression of circ_0008590 and its parent gene, reticuloendotheliosis viral oncogene related B (*RELB*) in human retinal microvascular endothelial cells (hRECs) in hyperglycemia and the potential mechanism.

Methods: The levels of *RELB*, circ_0008590, and miR-1243 in hRECs or clinical samples were detected by quantitative reverse transcription-polymerase chain reaction (qRT-PCR). Dual-luciferase reporter assay was used to test the interaction between *RELB*/circ_0008590 and miR-1243. Cell Counting Kit-8 (CCK-8), Transwell, flow cytometry (FCM), wound healing, and tube formation assays were used for the physiological investigation. The interaction between human *RELB* and circ_0008590 was studied in streptozotocin (STZ) induced diabetic retinopathy (DR) C57BL/6 mice.

Results: The levels of circ_0008590 and *RELB* were increased in hRECs in hyperglycemia; during the progression of DR, the levels of circ_0008590 and *RELB* messenger RNA (mRNA) in aqueous humor were first decreased and then increased, whereas miR-1243 showed an opposite trend. Both *RELB* 3'-untranslated region (UTR) and circ_0008590 shared a similar binding site for miR-1243. Further, miR-1243 mimic suppressed the proliferation and migration of hRECs, promoting the apoptosis ratio, which could be rescued by the overexpression of circ_0008590. In STZ-induced DR mice, miR-1243 agomir rescued the effects of the overexpression of human *RELB*.

Conclusions: In hyperglycemia, high expression of *RELB*/circ_0008590 could be suppressed by miR-1243, and the nuclear factor-κB (NF-κB) pathway is subsequently affected.

Keywords: Diabetic retinopathy (DR); hyperglycemia; reticuloendotheliosis viral oncogene related B (*RELB*); circ_0008590; miR-1243

Submitted Sep 24, 2021. Accepted for publication Nov 04, 2021.
doi: 10.21037/atm-21-5562
View this article at: https://dx.doi.org/10.21037/atm-21-5562

^ ORCID: 0000-0003-3477-4568.

Introduction

Diabetic retinopathy (DR) is a common complication of diabetes mellitus that is associated with chronic damage to the retinal microvasculature (1,2), which will lead to an increase of extracellular fluid and swelling of the retina and increase cell death, and almost always leads to vision loss (3). Recently, the global prevalence of DR has continued to increase (4). The available treatments for severe proliferative DR (PDR) include retinal laser therapy and intraocular microinjection of anti-vascular endothelial growth factor (VEGF) monoclonal antibodies; however, the recurrence rate is relatively high and the prognosis remains poor (5,6). The development of effective therapy protocols requires more systematic fundamental research on the progression of DR. Additionally, retinal microvasculature also plays vital roles in the development of retinoblastoma (Rb); it has been reported to be associated with the tumor growth and invasion, and anti-VEGF treatment could help to reduce tumor size and angiogenesis in Rb (7-9). To investigate the mechanism of retinal microvascularization and to screen the anti-angiogenesis pathway could help in the clinical diagnosis and therapy for associated eye diseases.

It has been reported that circular RNAs (circRNAs) can act as sponges for microRNAs (miRNAs) (10-12). In recent years, the number of studies of circRNAs in the field of DR has increased considerably: for example, circRNAs have been screened as potential biomarkers for DR (13); miR-1243 was shown to repress angiogenesis and inflammation in human retinal microvascular endothelial cells (hRECs) grown in a high-glucose environment by inhibiting hsa_circ_0002570 (12); circRNA COL1A2 promotes angiogenesis in DR (14); hsa_circ_0041795 induces ARPE-19 cell damage in a high-glucose environment by interacting with miR-646 (15); circRNA cPWWP2A promotes the DR-induced retinal vasculature by interacting with miR-579 (16), similar to other circRNAs, including circDNMT3B, circHIPK3, and circ_0005015 (17).

Nuclear factor-κB (NF-κB) plays vital roles in gene induction in a range of cellular responses, particularly throughout the immune system (18); usually, it is activated by the canonical and the noncanonical NF-κB signaling pathways. Both RELA and p50 play important roles in the canonical pathway, whereas reticuloendotheliosis viral oncogene related B (*RELB*), p100, and p52 are key elements in the noncanonical pathway (19,20). The canonical pathway has been well studied and is related to diseases such as autoimmunity, obesity, and cancer; in contrast, considerably less association has been reported between the noncanonical pathway and diseases and their associated pathology (21). Recently, as a subunit of the noncanonical NF-κB signaling pathway, RELB has been reported as highly expressed in diabetes mellitus (22), to promote the progression of uveal melanoma (23), associated with hyperoxic injury in fetal human pulmonary microvascular endothelial cells (24), and as essential for the survival of multiple myeloma (25). In addition, the overexpression of *RELB* could repress the interleukin-1 (IL-1)-induced production of inflammatory mediators in ocular fibroblasts (26). However, the involvement of *RELB* in DR has been seldom studied. As one circ RNA form of *RELB*, circ_0008590 is located at chr19 (45528586-45528995), and it is detected in RNA-sequencing of human tissue (27); however, circ_0008590 has seldom been studied in neovascularization associated diseases.

In this study, RNA-Seq was employed to screen differential circRNAs in hRECs cultivated in low- and high-glucose environments, and there was a significantly increasing of circ_0008590 under high-glucosecondition. Bioinformatics analysis suggested that circ_0008590 was a target of miR-1243, and that miR-1243 could also recognize a similar site in the 3'-untranslated region (UTR) of *RELB* messenger RNA (mRNA). The levels of circ_0008590, *RELB* mRNA, and miR-1243 were analyzed in aqueous humor samples from patients with DR; the relationships between these RNAs were investigated in hRECs and in a streptozotocin (STZ)-induced model of DR in C57BL/6 mice; and their roles in the pathogenesis of microvascular dysfunction were studied.

We present the following article in accordance with the ARRIVE reporting checklist (available at https://dx.doi.org/10.21037/atm-21-5562).

Methods

Clinical specimens

The study followed the tenets of the Declaration of Helsinki (as revised in 2013) and the Association for Research in Vision and Ophthalmology (ARVO) statement for research involving human subjects and was approved by the Ethics Committee of Nanjing Medical University (2014-062 and 2019-398). Aqueous humor samples from patients with non-proliferative DR (NPDR) (n=20), patients with PDR (n=22), and controls (patients without diabetes, n=20) were obtained from cataract surgery. Informed consent, written

in accordance with the ethical guidelines, was obtained from all participants. All samples were stored at –80 ℃ until RNA extraction. The clinical and histopathologic information was determined through a retrospective review of patient records.

Cell culture and reagents

The certified hRECs were purchased from the Cell Bank of the Chinese Academy of Science (Shanghai, China). These cells were cultivated in phenol red-free Dulbecco's Modified Eagle's Medium (DMEM; Lonza Inc., Morristown, NJ, USA). The high glucose (HG) and low glucose (LG) media were prepared as described in our previous work (28,29). The following antibodies were used in the experiments: anti-RELB (AB33907), anti-p100 (ab175192), and anti-p52 (ab129097), purchased from Abcam (Cambridge, MA, USA); and anti-Bcl-2 (15071), anti-Bax (89477), and anti-GAPDH (5174), purchased from Cell Signaling Technology (Beverly, MA, USA). Human/mouse *RELB* overexpression plasmid (OERELB, containing the 5'- and 3'-UTRs), siRELB (human) (5'-GCACAGAUGAAUUGGAGAUCA-3'), shRELB (mouse) (5'-ACCUCGACCUCUCUUCCCU GUCACUAUCAAGAGUAGUGACAGGGAAGAGA GGUCUU-3'), circ_0008590 overexpression plasmids (OECIRC) or adeno-associated viruses, or si-circ_0008590 (5'-CCCGUCUAUGACAAGAUUUUA-3') were synthesized by GenePharma (Suzhou, China). The miR-1243 mimics, inhibitors, and agomir were also purchased from GenePharma (Suzhou, China). Plasmids and RNAs were transfected into cells using Lipofectamine 2000 (Invitrogen, Carlsbad, CA, USA). A wound healing assay kit (ab242285) was purchased from Abcam (Cambridge, MA, USA). The hRECs were arranged into different groups including LG, HG, siRELB, HG + NC, OERELB, miR-1243 mimic, OERELB + miR-1243 mimic, siCIRC, OECIRC, and OECIRC + miR-1243 mimic; and in each physiological experiment, there were five parallel samples in each group.

RNA-Seq assay

We conducted RNA sequencing as described in our previous work (30). The raw data have been submitted to Gene Expression Omnibus-National Center for Biotechnology Information (GEO-NCBI; GSE117238). The data were screened by FastQC software (v0.11.9) and NGSQC software (v2.3.3) (31,32), the circRNAs were identified using Tophat2 (v2.1.1), Find_circ (v1.2), and CIRCexplorer2 software (33,34), and the differential expression of circRNAs between the HG and LG treatment was analyzed by the Limma (v3.44.3) package in R software (35).

Cell Counting Kit-8 (CCK-8) assay

In accordance with the manufacturer's protocol, hRECs were plated in 96-well plates (5,000 cells in 100 μL medium per well) 24 h before the experiment, and cell proliferation was then investigated using a CCK-8 kit (Dojindo Laboratories, Kumamoto, Japan) (28,29). Each experiment was repeated 5 times.

Transwell migration assay

To investigate the migration of hRECs, a Transwell chamber with an 8 μm polycarbonate pore membrane was employed. The hRECs were transferred to serum-free DMEM for 6 h. Subsequently, the cells exposed to different environments were seeded in the upper wells (4.0×10^4 cells/200 μL serum-free DMEM), and the lower wells were filled with 800 μL DMEM containing 20% fetal bovine serum (FBS). After 6 h, the hRECs that had migrated across the filter were fixed in 4% paraformaldehyde and stained with crystal violet. The cells in three random fields per well were counted under 100× magnification using a light microscope (Nikon, Tokyo, Japan) (28,29). Each experiment was repeated 5 times.

Scratch-wound assay

Using a wound healing assay kit (ab242285), hRECs were plated in the wells and grown to confluence, the inserts of the kit created a defined gap, and then wound healing over 24 h was monitored. To calculate the relative wound density (RWD) of the cells, the photos were analyzed using IncuCyte ZOOM software (ESSEN BioScience, Ann Arbor, MI, USA) (28,29). Each experiment was repeated 5 times.

Tube formation assay

After basement membrane matrix (BD Biosciences) was placed into a 24-well plate and incubated at 37 ℃ for 0.5 h, hRECs were seeded into each well, and tube formation was observed over 4 h at 37 ℃ by using an Olympus IX-73 microscope (28,29). Each experiment was repeated for 5 times.

Table 1 Primers for qRT-PCR assay

Target	Primers
Circ_0008590	F: 5'-GGTGAGGATCTGCTTCCAGG-3'
	R: 5'-GATGGTTCTTCAGGGACCCA-3'
RELB	F: 5'-GGCATTGACCCCTACAACG-3'
	R: 5'-GGCTCGGAAAGCACAGG-3'
miR-1243	F: 5'-GTCAACTGGATCAA TTATAGG-3'
	R: 5'-GTGCAGGGTCCGAGGT-3'
Cel-miR-39-3p	F: 5'-GTCACCGGGTGTAAATCAG-3'
	R: 5'-GGTCCAGTTTTTTTTTTTTTTTCAAG-3'
GAPDH	F: 5'-GCACCGTCAAGGCTGAGAAC-3'
	R: 5'-TGGTGAAGACGCCAGTGGA-3'

qRT-PCR, quantitative reverse transcription-polymerase chain reaction.

Western blotting analysis

After cells were lysed, the extracted proteins were quantified using a Pierce™ BCA Protein Assay Kit (Thermo Fisher, Waltham, MA, USA). Equal amounts of protein were loaded onto a 12% sodium dodecyl sulfate-polyacrylamide gel electrophoresis (SDS-PAGE) gel using a NuPAGE system (Invitrogen) and then transferred onto polyvinylidene fluoride (PVDF) membranes as previously described (28,29).

Quantitative reverse transcription-polymerase chain reaction (qRT-PCR) analysis

As described in our previous work (28,29), the total RNAs and total miRNAs were extracted, and the levels of *RELB* mRNA and circ_0008590 in hRECs and aqueous humor were detected using Moloney murine leukemia virus (M-MLV) reverse transcriptase (Invitrogen) and SYBR Green RealTime PCR Master Mix. GAPDH was used as the internal control. The level of miR-1243 was detected using the mirVana™ qRT-PCR miRNA detection kit from Invitrogen, with cel-miR-39-3p spike-in used as the internal control. The primers were designed using the OligoArchitect™ Online service (https://www.sigmaaldrich.com/china-mainland/zh/ technical-documents/articles/biology/oligoarchitect-online.html) and miRprimer (https://sourceforge.net/projects/mirprimer/), and were synthesized by GenePharma (Shanghai, China) (*Table 1*).

Flow cytometry (FCM) experiments

The Annexin V/FITC kit [Becton, Dickinson, and Co., (BD) Biosciences, San Jose, CA, USA] was employed to label apoptotic cells in accordance with the manufacturer's instructions, and the cells were monitored by FCM. The hRECs were digested with trypsin without ethylenediamine tetraacetic acid (EDTA), and then were collected in medium and precipitated by a 5 min centrifugation at 500 ×g. After being washed and resuspended with 1× binding buffer, hRECs were mixed with 5 μL annexin V-FITC, and further incubated in the dark at room temperature for 10 min. The hRECs were stained with 10 μL of propidium iodide (PI; 20 μg/mL) for 5 min in the dark, and finally applied for florescent detection. Each experiment was repeated 3 times.

Dual-luciferase reporter assay

The pGL3-luc plasmids containing luciferase reporter gene and wild/mutated circ_0008590 or *RELB* 3'-UTR and miR-1243 were synthesized by GenePharma (Shanghai, China). The Lipofectamine 2000 transfection system was used for transient transfections, the firefly luciferase activity and the Renilla activity were determined with a luminometer using the Dual Luciferase Assay System (Promega, Madison, WI, USA) (28,29). Each experiment was repeated 5 times.

DR mouse model

All animal experiments adhered to institutional guidelines for humane treatment of animals, the Principles of Laboratory Animal Care (National Institutes of Health, Bethesda, MD, USA), and the ARVO Statement for the Use of Animals in Ophthalmic and Vision Research. The animal experiments were approved by the Ethics Committee of Nanjing Medical University (2019-398 approved on 25 February 2019).

The C57BL/6 mice were obtained from Changzhou Cavens Laboratory Animals Co., Ltd. and were housed in the specific-pathogen-free (SPF) animal center of the Affiliated Wuxi People's Hospital of Nanjing Medical University at 22.5 ℃ and 42.5% humidity with a 12 h/12 h light-dark cycle; heated wood chip litter was used as bedding material, and ad libitum consumption of food and water were permitted. The mice were randomly

arranged. As previously reported, 50 μg/g STZ was injected intraperitoneally for 5 days continuously into 8-week-old male C57BL/6 mice (weight 24.8±1.2 g), with citrate buffer used as a blank. The model was considered successfully established when the blood glucose level in the mice exceeded 16.7 mmol/L (36). After intraperitoneal injection of 80 μg/g ketamine and 4 μg/g xylazine, the mice were ventilated, and approximately 1.5 μL (1×10^{12} TU/mL) of adeno-associated virus containing mouse/human *RELB* complementary DNA (cDNA) with the 5'- and 3'-UTR were intravitreally injected. To maximize virus delivery, the mice were administered an intravitreal injection once per month. For the short-hairpin RNA (shRNA) adenovirus and miR-1243 agomir, the mice were administered an intravitreal injection (2 nmol in 50 μL stroke-physiological saline solution) every 2 weeks (37,38). The mice were arranged into different groups, including: normal, STZ, NC, STZ + miR-1243 agomir, STZ + OE mouse *RELB*, STZ + mouse *RELB* shRNA, STZ + OE human *RELB*, and STZ + OE human *RELB* + miR-1243 agomir, with 5 mice in each group. After 15–16 weeks, Evans blue leakage and retinal trypsin digestion assays were performed as described in our previous work (36). After trypsin digestion, pericytes and hRECs were counted (37), and the thickness of the basement membrane was detected using a reported protocol (39,40).

Statistical analysis

All data were presented as the mean ± SD. All *in vitro* experiments were repeated at least 3 times. The data were analyzed using the software SPSS 13.0 (IBM Corp., Chicago, IL, USA); the *t*-test was used for comparisons between two groups, and one-way analysis of variance (ANOVA) was used for comparisons of more than two groups. We considered P values of <0.05 statistically significant.

Results

Circ_0008590 and RELB mRNA levels in hRECs and the aqueous humor

The hRECs were cultivated in HG and LG medium and then analyzed by RNA-Seq and qRT-PCR. In the RNA-Seq analysis, 17,541 circRNAs were detected. In 6 samples from the two groups, 98 differentially expressed circRNAs were identified, and circ_0008590, a circRNA form of *RELB*, was significantly increased in expression in cells grown in HG medium (*Figure 1A-1C*). The levels of circ_0008590 and *RELB* in hRECs and the aqueous humor of patients with DR and the normal controls were then investigated by qRT-PCR. In hRECs grown in HG medium, the levels of circ_0008590 and *RELB* mRNA were increased (*Figure 1D*). During the progression of DR, circ_0008590 and *RELB* followed similar fluctuations; they were decreased in the aqueous humor samples from participants with NPDR, and then significantly increased in those with PDR (*Figure 1E*).

Direct interaction between circ_0008590/RELB and miR-1243

To investigate the possible relationship between circ_0008590/*RELB* and miR-1243, the sequences were analyzed using the NIH Circular RNA Interactome online service (https://circinteractome.nia.nih.gov/mirna_target_sites.html) and the TargetScanHuman online service (https://www.targetscan.org/vert_70/); the potential binding sites in circ_0008590 (17-23) (*Figure 2A*), and in the 3'-UTR of *RELB* (272–278) (*Figure 2B*) were predicted as the target sites of miR-1243. To confirm the interaction between circ_0008590/*RELB* and miR-1243, wild-type (WT) and mutant (MUT) forms of the predicted target sites in circ_0008590 or *RELB* mRNA 3‘-UTR were transfected into hRECs, respectively. The transient co-transfection of hRECs with WT reporter plasmids and miR-1243 mimics all resulted in reduced luciferase activity, whereas transfection of the MUT plasmids did not (*Figure 2C*,*2D*). In addition, the level of miR-1243 was reduced in hRECs grown in HG medium (*Figure 1D*), but followed an opposite trend to circ_0008590 and *RELB* mRNA during the progression of DR (*Figure 1E*).

Effects of RELB on the proliferation, migration, and apoptosis of hRECs

To investigate the effects of *RELB* on hRECs, siRNA sequences targeting *RELB* mRNA (siRELB) or scrambled negative control siRNA (siNC) were transfected into hRECs grown in an HG environment. After knockdown of *RELB* expression, the proliferation of hRECs was decreased (*Figure 3A*), whereas the proportion of dead cells and apoptotic cells was increased (*Figure 3B*); additionally, as shown by the Transwell and wound healing assays

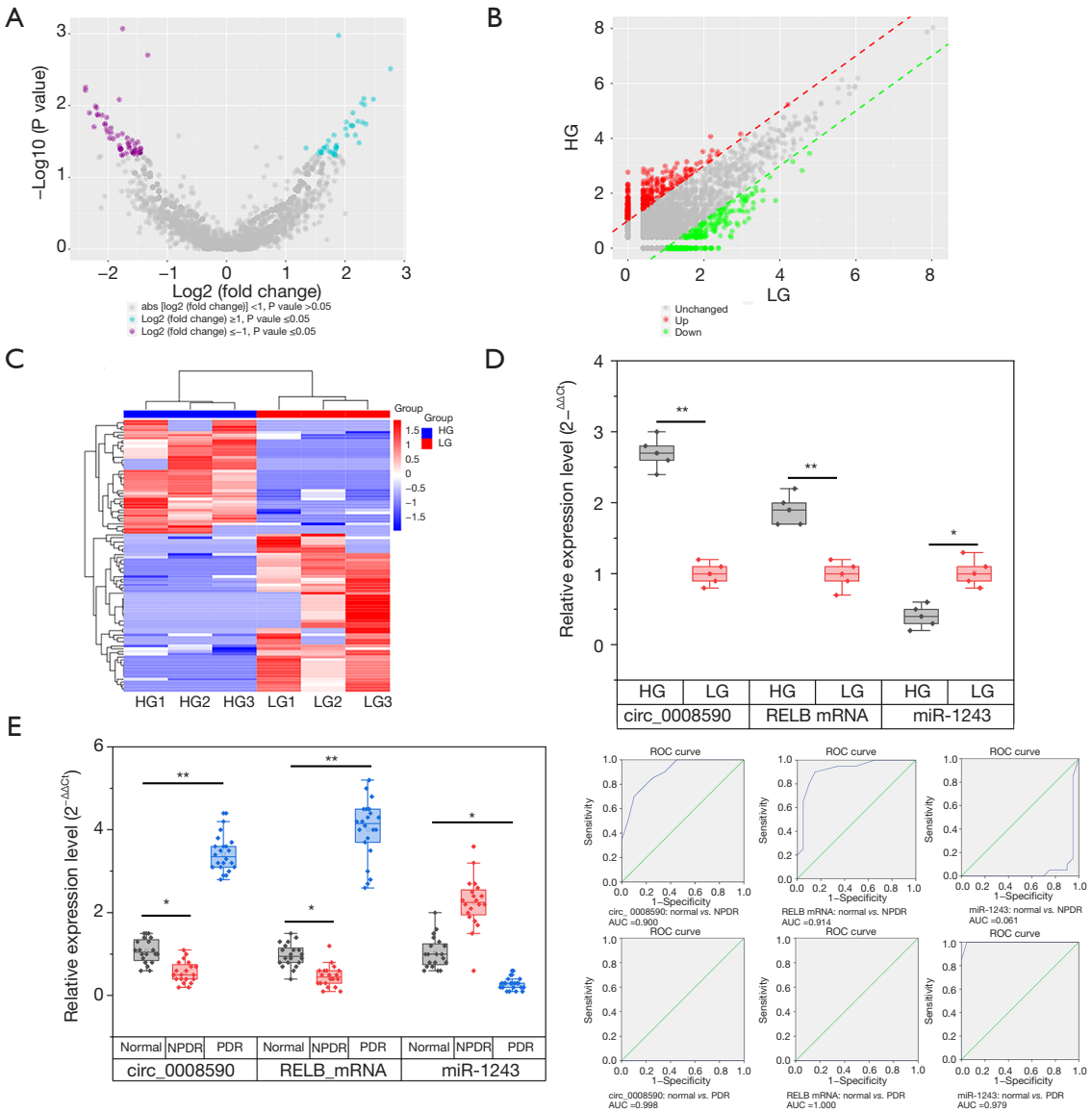

Figure 1 Screening of differential circRNAs and associated targets for DR. From the RNA-Seq analysis: (A) volcano plot displaying the dysregulated circRNAs between HG and LG environments. The blue points represent significantly upregulated circRNAs in the HG group, and the purple points represent significantly downregulated circRNAs in the HG group. (B) Scatter plot presenting the variation in circRNA expression between the HG and LG groups. The values on the X and Y axes represent the normalized circRNA signal values (log2 scale). The red points are the upregulated circRNAs and the green points are the downregulated circRNAs. (C) Heatmap of inter-sample correlation showing the differential circRNA expression levels between the HG and LG groups. Pearson's correlation coefficients are presented on a color scale. The intensity increased from blue (relatively low correlation) to red (relatively high correlation). The correlation was evaluated by Pearson's correlation coefficient of significantly differential circRNA expression levels. The expression level of circ_0008590 was significantly increased in the HG group. (D) The expression levels of circ_0008590/*RELB* mRNA and miR-1243 were detected in hRECs cultivated in an HG or an LG environment. (E) The expression levels of circ_0008590/*RELB* mRNA and miR-1243 were detected in aqueous humor samples from patients with NPDR (n=20), patients with PDR (n=22), and normal controls (n=20). *, P<0.05; **, P<0.01. Logistic regression models and ROC curves were constructed: the AUCs of circ_0008590 (normal *vs.* NPDR and normal *vs.* PDR) were 0.900 and 0.998, the AUCs of *RELB* mRNA (normal *vs.* NPDR and normal *vs.* PDR) were 0.914 and 1.000, and the AUCs of miR-1243 (normal *vs.* NPDR and normal *vs.* PDR) were 0.061 and 0.979, respectively. CircRNA, circular RNA; DR, diabetic retinopathy; HG, high glucose; LG, low glucose; *RELB*, reticuloendotheliosis viral oncogene related B; mRNA, messenger RNA; hRECs, human retinal microvascular endothelial cells; NPDR, non-proliferative DR; PDR, proliferative DR; ROC, receiver operating characteristic; AUC, area under the curve.

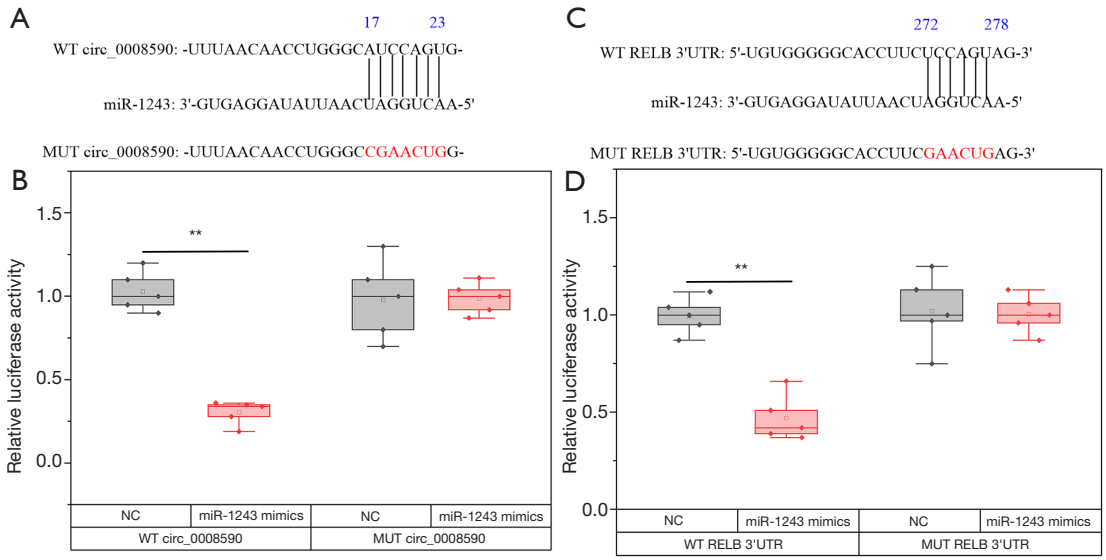

Figure 2 Circ_0008590 and *RELB* mRNA 3'-UTR are targets of miR-1243. (A) Binding region between circ_0008590 and miR-1243. (B) The luciferase reporter constructs containing the WT circ_0008590 or MUT circ_0008590 sequence were co-transfected with miR-1243 mimic or the corresponding negative controls, respectively. (C) Binding region between the *RELB* mRNA 3'-UTR and miR-1243. (D) The luciferase reporter constructs containing the WT *RELB* mRNA 3'-UTR or MUT *RELB* mRNA 3'-UTR sequences were co-transfected with miR-1243 mimic or the corresponding negative controls, respectively. Three independent experiments were performed. Error bars show the mean ± SD of at least three repeat experiments. **, P<0.01. *RELB*, reticuloendotheliosis viral oncogene related B; mRNA, messenger RNA; UTR, untranslated region; WT, wild-type; MUT, mutant.

(*Figure 3C-3E*), the migration of hRECs was decreased, whereas tube formation was suppressed (*Figure 3F,3G*). As shown by the western blotting analysis, in hRECs transfected with siRELB, the levels of RELB, p52, and Bcl-2 were decreased, whereas the level of Bax, a key effector of cell apoptosis, was increased (*Figure 3H*).

Mutual inhibition of RELB mRNA and miR-1243 in hRECs

It has been reported that miRNAs act as sponges for target mRNAs that can subsequently regulate the expression of their target genes. In this work, a potential binding site of miR-1243 was identified in the 3‘-UTR region of *RELB* mRNA. To investigate whether miR-1243 mimic could regulate the level of *RELB* in hRECs, a *RELB* overexpression plasmid (OERELB containing the 5'- and 3'-UTR), siRELB, and miR-1243 mimics were transfected or co-transfected into hRECs, and the cells were then cultivated in HG medium. The knockdown of *RELB* mRNA increased the level of miR-1243, whereas the overexpression of *RELB* mRNA slightly suppressed miR-1243; in contrast, the level of *RELB* mRNA was increased by the inhibition of miR-1243 and decreased by the presence of miR-1243 mimic (*Figure 4A*). In addition, as shown by CCK-8 (*Figure 4B*), FCM (*Figure 4C,4D*), Transwell (*Figure 4E*), wound healing (*Figure 4F,4G*), and tube formation (*Figure 4H,4I*) assays, miR-1243 mimic and *RELB* knockdown promoted apoptosis and cell death in hRECS and repressed proliferation, migration, wound healing, and tube formation; in contrast, the overexpression of *RELB* slightly reduced the proportion of apoptotic cells and reversed the effects of the miR-1243 mimic on hRECs.

Circ_0008590 reversed the effects of miR-1243

Given the predicted interaction between circ_0008590 and miR-1243, to evaluate whether circ_0008590 could reverse the effects of miR-1243 in DR, circ_0008590 overexpression plasmid (OECIRC), si-circ_0008590 (siCIRC), siNC, and miR-1243 mimic were co-transfected into hRECs, and the cells were grown in HG medium. The overexpression of circ_0008590 increased the level of *RELB* mRNA,

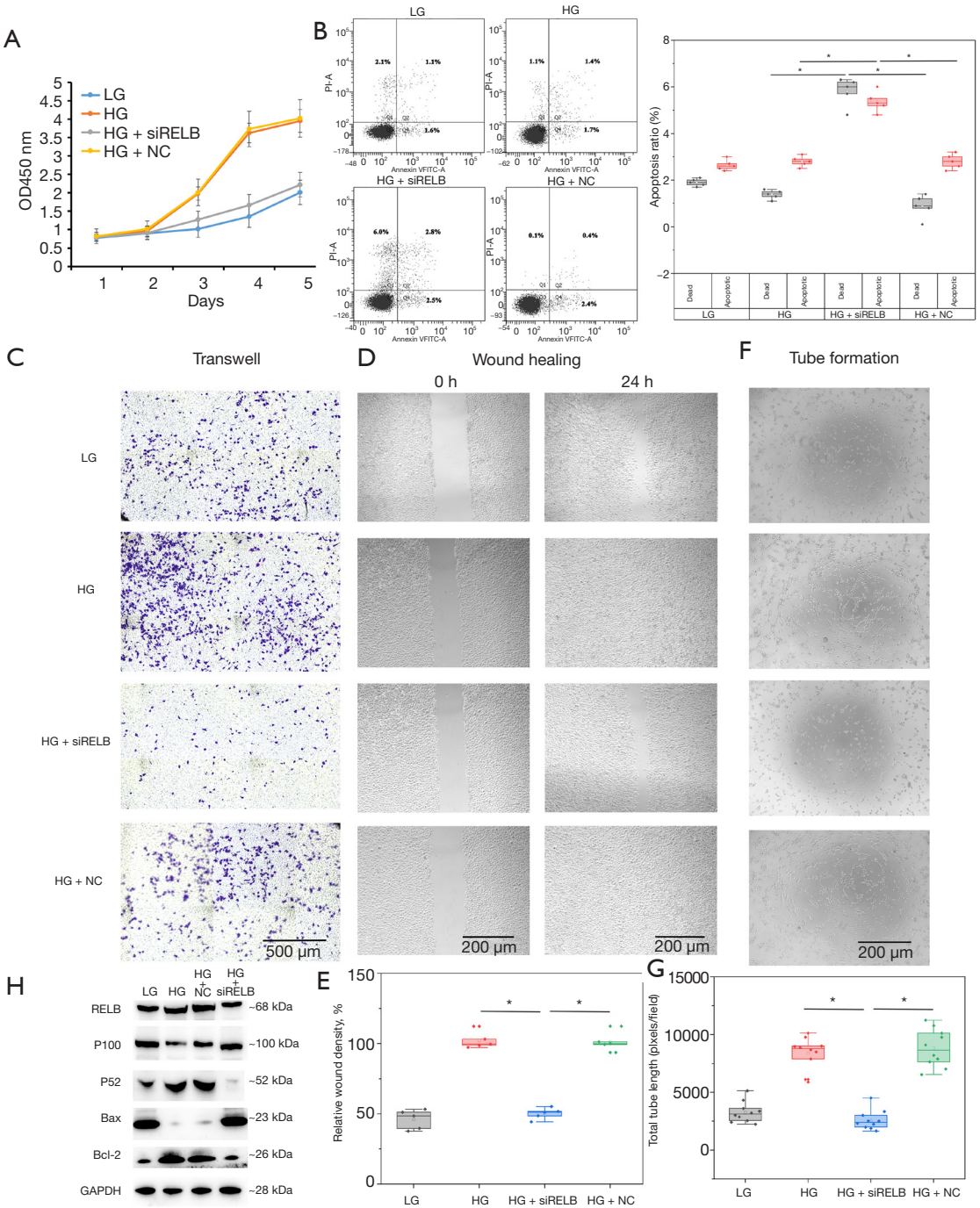

Figure 3 *RELB* affects proliferation, apoptosis, and migration in hRECs. (A) CCK-8 analysis showing that *RELB* knockdown inhibited the proliferation of hRECs. (B) FCM analysis showing that after transfection with siRELB, apoptosis and cell death significantly increased in hRECs. (C) As shown by the Transwell assay, the cells were stained with crystal violet; the knockdown of *RELB* repressed the migration of hRECs, the scale bar was 500 μm. (D,E) Transfection with siRELB reduced the wound healing process, the scale bar was 200 μm. (F,G) siRELB decreased the tube formation process, the scale bar was 200 μm. Error bars represent the mean ± SD of at least triplicate experiments. *, P<0.05. (H) Western blotting analysis of protein levels of RELB, p100, p52, Bax, and Bcl-2. After transfection with siRELB, the protein level of *RELB* was decreased, whereas that of p100 was increased and p52 was decreased; for proteins in the canonical apoptosis pathway, Bcl-2 was decreased and the level of Bax was increased. RELB, reticuloendotheliosis viral oncogene related B; hRECs, human retinal microvascular endothelial cells; CCK-8, Cell Counting Kit-8; FCM, flow cytometry; HG, high glucose; LG, low glucose.

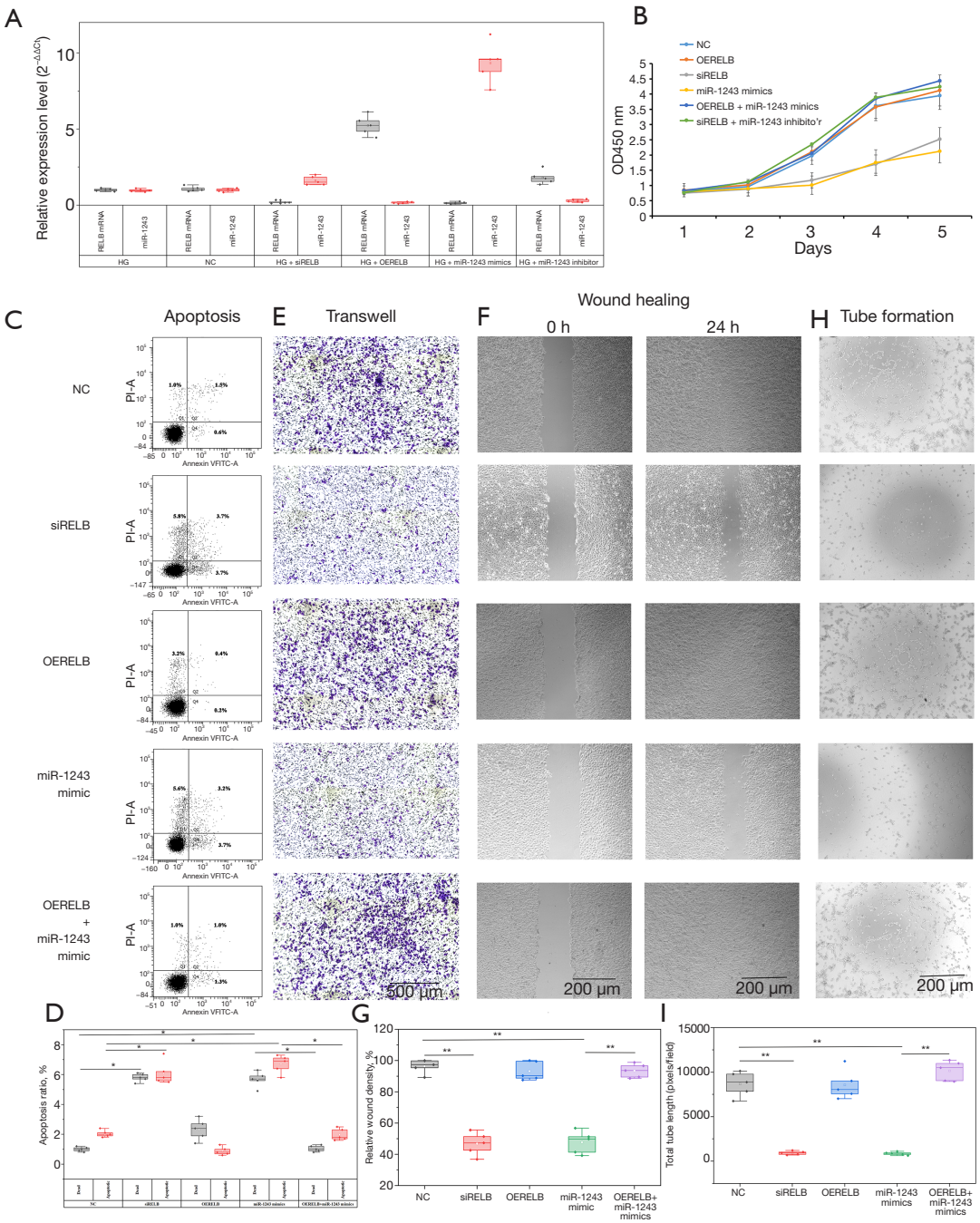

Figure 4 Mutual inhibition of *RELB* and miR-1243. (A) qRT-PCR analysis showing that the overexpression of *RELB* mRNA resulted in the inhibition of miR-1243, and vice versa; similarly, the knockdown of *RELB* mRNA resulted in the upregulation of miRNA-1243, and vice versa. (B) CCK-8 analysis showing that miR-1243 mimics repressed the proliferation of hRECs, and that the overexpression of *RELB* could reverse this phenomenon. (C,D) Transfection with miR-1243 mimic or siRELB significantly increased the proportion of apoptotic hRECs, and the overexpression of *RELB* reversed the effects of miR-1243. In addition, miR-1243 significantly suppressed (E) migration (the cells were stained with crystal violet, the scale bar was 500 μm), (F,G) wound healing (the scale bar was 200 μm), and (H,I) tube formation (the scale bar was 200 μm) in hRECs; however, the overexpression of *RELB* significantly reversed these trends. The error bars represent the mean ± SD of at least triplicate experiments. *, P<0.05; **, P<0.01. *RELB*, reticuloendotheliosis viral oncogene related B; qRT-PCR, quantitative reverse transcription-polymerase chain reaction; mRNA, messenger RNA; CCK-8, Cell Counting Kit-8; hRECs, human retinal microvascular endothelial cells.

resulting in similar inhibition of miR-1243 as *RELB*; circ_0008590 knockdown resulted in the opposite effect. In contrast, the level of circ_0008590 was promoted by the knockdown of miR-1243, but decreased by the transfection of miR-1243 mimic (*Figure 5A*). Furthermore, as shown by CCK-8 (*Figure 5B*), FCM (*Figure 5C,5D*), Transwell (*Figure 5E*), wound healing (*Figure 5F,5G*), and tube formation (*Figure 5H,5I*) assays, miR-1243 mimic or cire_0008590 knockdown significantly promoted apoptosis and cell death and repressed proliferation, migration, wound healing, and tube formation in hRECs, whereas the overexpression of circ_0008590 reversed the effects of miR-1243 mimic on hRECs.

miR-1243 rescued the function of overexpressed human RELB in DR mice

According to the miRbase online service (https://www.mirbase.org/index.shtml), miR-1243 is only found in human cells, with no similar miRNAs present in rats or mice. In addition, TargetScanHuman online service indicated that the 3'-UTR of human or mouse *RELB* mRNA was not conserved, and the miR-1243-recognized target could not be found in mice (*Figure 6A*). Furthermore, according to the NIH Circular RNA Interactome online service and circBase online service, circ_0008590 is only expressed in human cells, with no similar sequences in rats or mice. The alignment of the amino acid sequences revealed that the sequence identity and similarity between mouse RELB (NCBI Reference Sequence: NP_033072.2) and human RELB (NCBI Reference Sequence: NP_006500.2) were 88.7% and 92.6%, respectively (*Figure 6B*), suggesting that human RELB may exhibit a similar function to mouse RELB *in vivo*.

As shown in *Figure 7A,7B*, the retinal vascular leakage of normal mice (8.9%±3.2%, 3/10 eyes) was significantly lower than that in the STZ-induced DR mice (32.3%±3.5%, 3/10 eyes), the STZ induced NC mice (34.8%±4.4%, 3/10 eyes), and mice treated with *RELB* shRNA (18.5%±2.0%, 3/10 eyes), whereas miR-1243 agomir (37.4%±4.0%, 3/10 eyes) resulted in no significant difference in retinal vascular leakage in DR mice. The overexpression of mouse *RELB* and human *RELB* resulted in continuing deterioration of retinal vascular leakage to 58.4%±3.1% (3/10 eyes) and 55.0%±5.4% (3/10 eyes), respectively; but treatment with miR-1243 agomir significantly rescued the effects of the overexpression of human *RELB*, and the retinal vascular leakage was reduced to 34.3%±4.8% (3/10 eyes).

After trypsin digestion, as shown in *Figure 7C,7D*, the number of acellular capillaries in 10 fields of the retina was increased from 30.7±6.3 (normal mice, 4/10 eyes) to 116.7±18.0 (DR mice, 4/10 eyes) and 111.3±11.3 (STZ induced NC mice, 4/10 eyes); in mice treated with *RELB* shRNA (51.3±9, 4/10 eyes), the number of acellular capillaries was significantly reduced, whereas miR-1243 agomir (134±15, 4/10 eyes) did not significantly affect the number of acellular capillaries difference in DR mice. The overexpression of mouse *RELB* (217.0±23.7, 4/10 eyes) and human *RELB* (212.0±16.8, 4/10 eyes) resulted in further deterioration, and treatment with miR-1243 agomir (98.2±8.5, 4/10 eyes) only partially reversed the effects of the overexpression of human *RELB*.

In addition, as shown in *Figure 7C,7E*, in the retina of control mice, the ratio of hRECs to pericytes per square millimeter was 2.6±0.5 (4/10 eyes); owing to the loss of pericytes during DR, the ratio was increased to 9.7±0.7 (4/10 eyes) and 8.9±1.9 (4/10 eyes) in STZ-induced DR mice and STZ-induced NC mice, respectively; *RELB* shRNA (4.4±0.7, 4/10 eyes) significantly reduced the ratio, whereas miR-1243 agomir (9.9±1.8, 4/10 eyes) resulted in no significant difference in DR mice. The overexpression of mouse *RELB* (14.6±1.3, 4/10 eyes) and human *RELB* (14.9±0.9, 4/10 eyes) resulted in further deterioration, and treatment with miR-1243 agomir (10.3±1.0, 4/10 eyes) only partially reversed the effects of the overexpression of human *RELB*.

Compared with normal mice (0.31±0.09 μm, 3/10 eyes), the basement membrane was thicker in STZ-induced DR mice and STZ-induced NC mice, at 0.85±0.15 (3/10 eyes) and 0.84±0.15 (3/10 eyes) μm, respectively; mouse *RELB* shRNA (0.38±0.06 μm, 3/10 eyes) significantly reduced the thickness, and miR-1243 agomir (0.72±0.15 μm, 3/10 eyes) had no significant effect in DR mice. The overexpression of mouse *RELB* (1.95±0.16 μm, 3/10 eyes) and human *RELB* (1.74±0.19 μm, 3/10 eyes) resulted in continuing deterioration, and treatment with miR-1243 agomir (0.72±0.15 μm, 3/10 eyes) partially reversed the effects of the overexpression of human *RELB* (*Figure 7F,7G*).

The overexpression of mouse *RELB* significantly promoted retinal vascular leakage and neovascularization, whereas knockdown of mouse *RELB* resulted in the opposite effects. Unexpectedly, the overexpression of human *RELB* caused the same effects as the overexpression of mouse *RELB*, although these effects could be rescued by the co-

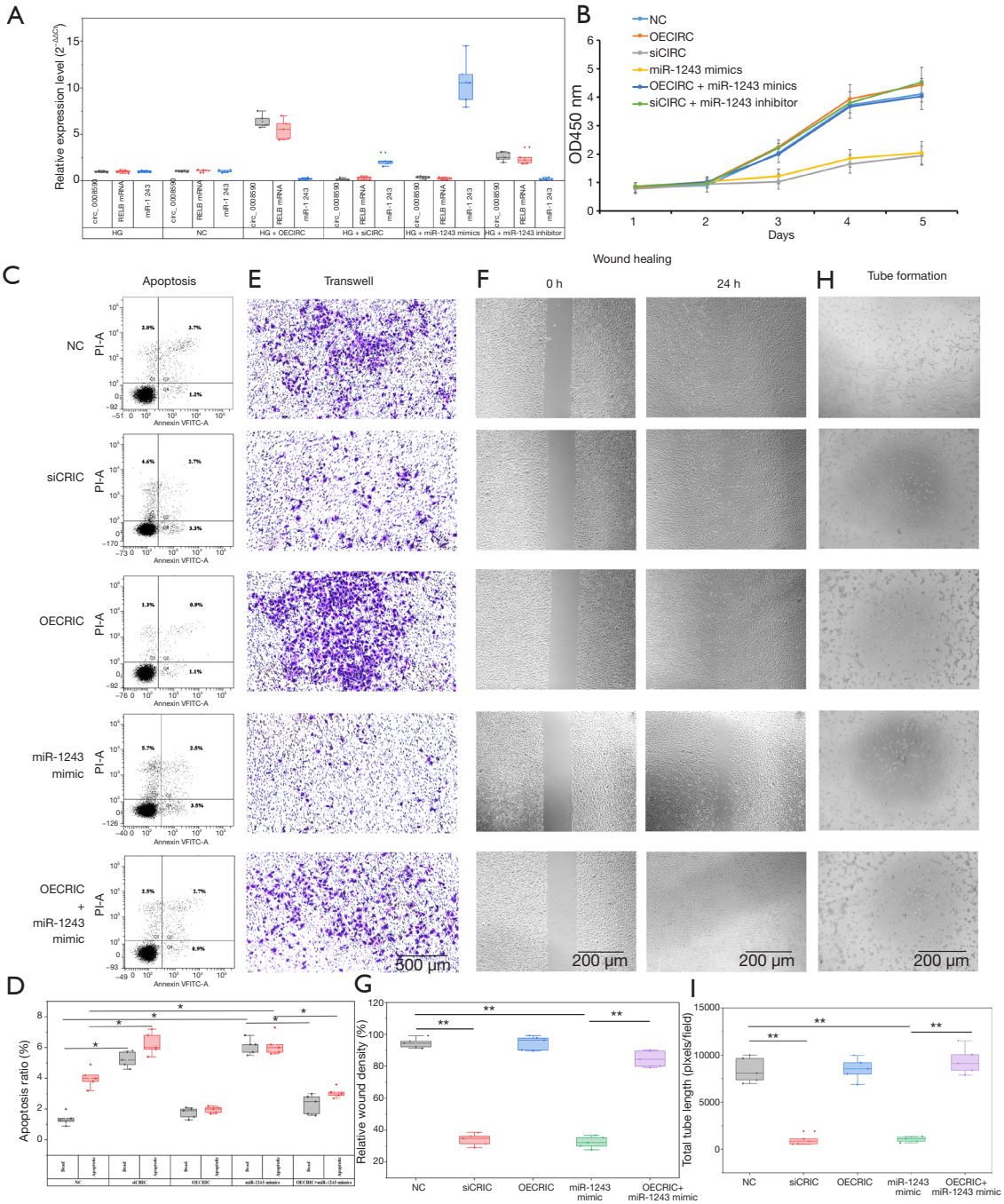

Figure 5 Circ_0008590 reverses effects of miR-1243. (A) The overexpression of circ_0008590 increased the level of *RELB* mRNA and suppressed the level of miR-1243, whereas knockdown of circ_0008590 led to a decrease in *RELB* mRNA and an increase in miR-1243. miR-1243 mimics suppressed the levels of *RELB* mRNA and circ_0008590, whereas the miR-1243 inhibitor resulted in the opposite effect. In (B) CCK-8, (C,D) FCM, (E) Transwell (the cells were stained with crystal violet, the scale bar was 500 μm), (F,G) wound healing (the scale bar was 200 μm), and (H,I) tube formation assays (the scale bar was 200 μm), knockdown of circ_0008590 conferred similar effects to *RELB* mRNA on proliferation, apoptosis, migration, and tube formation in hRECs. In addition, the overexpression of circ_0008590 also reversed the effects of miR-1243 mimics on hRECs. The error bars represent the mean ± SD of at least triplicate experiments. *, P<0.05; **, P<0.01. *RELB*, reticuloendotheliosis viral oncogene related B; mRNA, messenger RNA; CCK-8, Cell Counting Kit-8; FCM, flow cytometry; hRECs, human retinal microvascular endothelial cells.

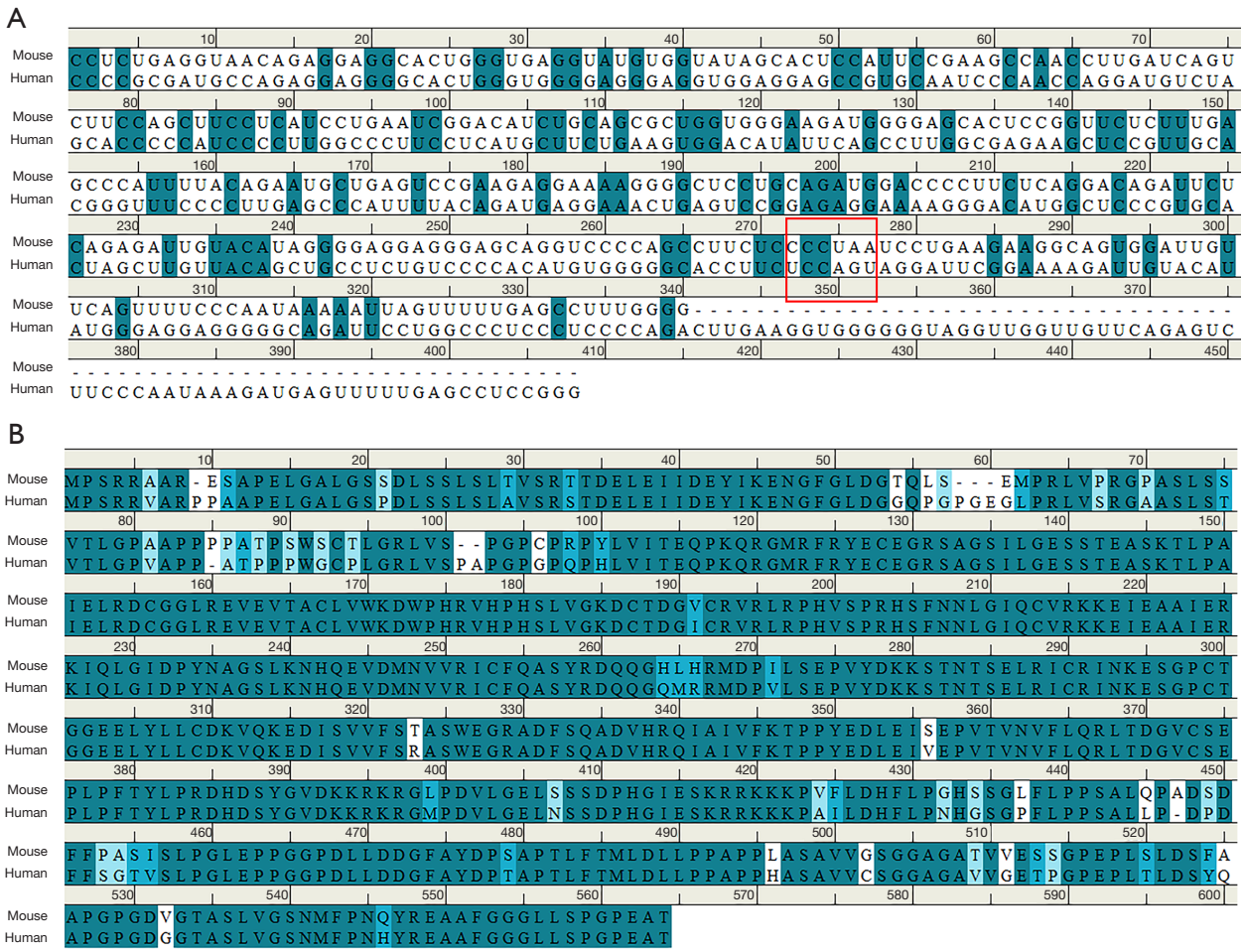

Figure 6 Sequence alignment. (A) The 3'-UTR of mouse and human *RELB* mRNA is not conserved. The recognition site of miR-1243 is marked by a red rectangle. (B) The mouse and human RELB amino acid sequences have high homology, with 88.7% identity and 92.6% similarity. UTR, untranslated region; *RELB*, reticuloendotheliosis viral oncogene related B; mRNA, messenger RNA.

injection of miR-1243 agomir. However, the injection of miR-1243 agomir alone had no effects, which was likely due to the lack of a target site.

Discussion

It has been identified that circRNAs are an important regulator of transcription and expression, mediating their effects by binding to the restriction sites on target mRNA or miRNAs. However, in recent years, "sponging" between circRNAs and miRNAs has been a hot topic for researchers studying genetic regulation (10). In this study, the RNA-Seq analysis indicated that there was a significant increase in circ_0008590, a circRNA form of *RELB*, in hRECs cultivated in an HG environment. Through qRT-PCR analysis, the levels of *RELB* mRNA and circ_0008590 were investigated. Under HG conditions, *RELB* mRNA and circ_0008590 were increased in hRECs; however, in the aqueous humor samples from participants with DR, the levels of *RELB* mRNA and circ_0008590 were decreased in the NPDR group, but were significantly increased in the DR group. The RELB is a key factor in the noncanonical pathway; it is known to protect against apoptosis in inflammation (19,20), and has been reported as associated with various diseases, including diabetes mellitus (22), uveal melanoma (23), hyperoxic injury of fetal human pulmonary microvascular endothelial cells (24), and multiple myeloma (25).

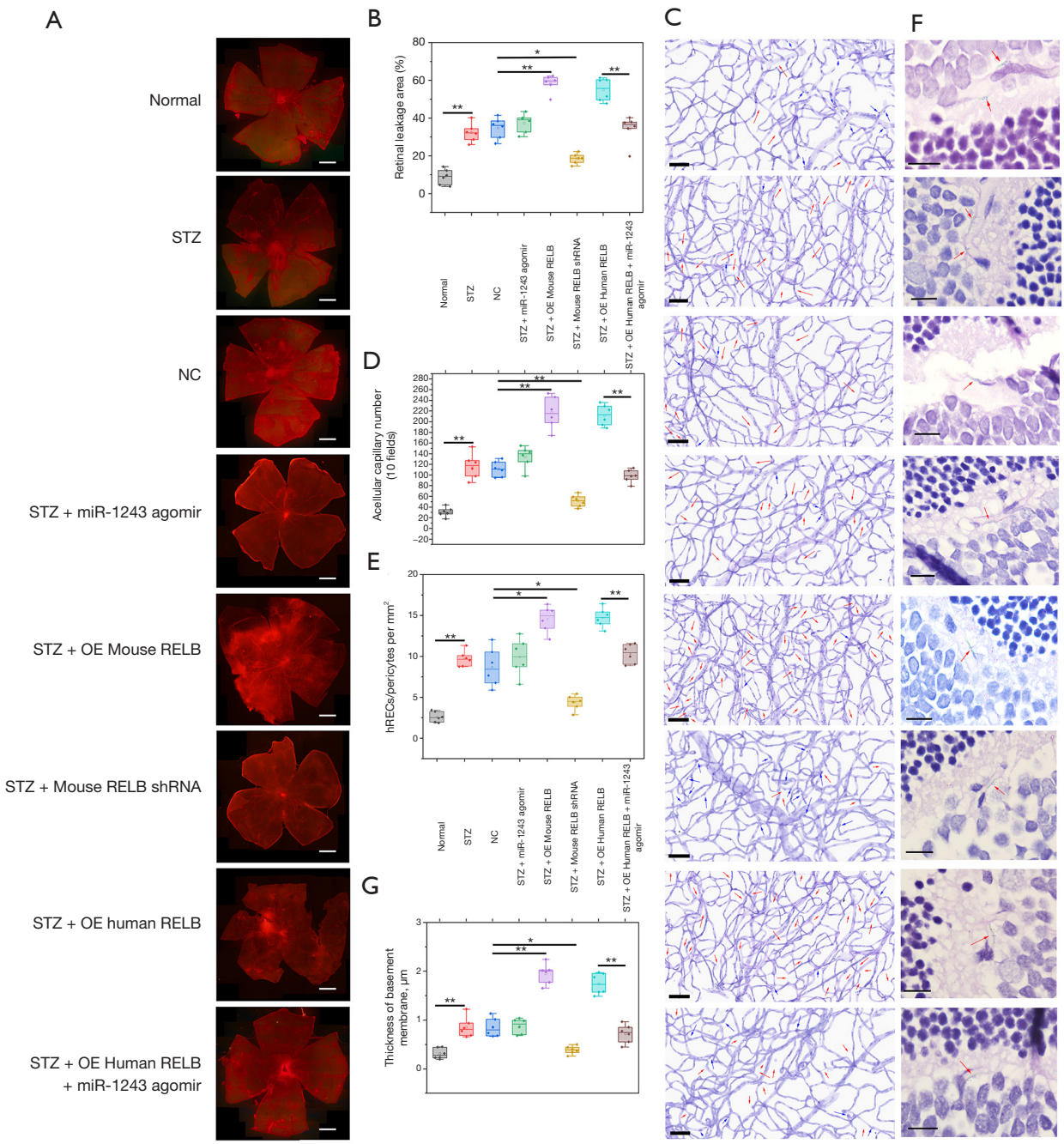

Figure 7 Interaction between human *RELB* mRNA and miR-1243 in mouse model of DR. (A,B) The Evans blue assay was used for the detection of retinal vascular leakage, the retina was stained with Evans blue, and the scale bar was 500 μm; the leakage area was calculated. (C) PAS staining was used after retinal trypsin digestion, the numbers of acellular capillaries, hRECs, and pericytes were counted (acellular capillaries are marked by red arrows, and pericytes are marked by blue arrows; scale bar =60 μm). (D) The number of acellular capillaries in 10 fields. (E) The hRECs/pericytes ratio in 1 mm^2. (F) Ultrathin sections of the retina were fixed in osmium tetroxide, embedded in epoxy resin, stained with HE, and the thickness of the basement membrane was measured (the basement membrane is marked by red arrows; scale bar =10 μm). (G) The thickness of basement membrane in 10 fields. The error bars represent the mean ± SD of at least triplicate experiments. *, P<0.05; **, P<0.01. *RELB*, reticuloendotheliosis viral oncogene related B; mRNA, messenger RNA; DR, diabetic retinopathy; PAS, periodic acid Schiff; hRECs, human retinal microvascular endothelial cells; HE, hematoxylin-eosin.

As the inflammatory process is reportedly involved in DR (41,42), we aimed to determine the mechanism for the abnormal fluctuation of *RELB* mRNA and circ_0008590 in hRECs and aqueous humor samples from patients with DR.

From screening using the NIH Circular RNA Interactome online service and TargetScanHuman online service, the miRNA miR-1243 was predicted to bind with circ_0008590 (17-23) or the 3‘-UTR of *RELB* mRNA (272–278), recognizing similar sites; and in hRECs, the direct interaction between circ_0008590 and miR-1243 or the *RELB* mRNA 3'-UTR and miR-1243 was confirmed using dual-luciferase reporter assays. The results indicated that there should be a collaborative relationship between circ_0008590/*RELB* against miR-1243. In this work, in hRECs cultivated in a HG environment, the overexpression of *RELB* mRNA did not affect proliferation, migration, wound healing, and tube formation processes, although the proportion of apoptotic cells was slightly reduced; however, *RELB* knockdown promoted apoptosis by regulating the downstream factors, such as p100, p52, Bax, and Bcl-2, which are important effectors of cell apoptosis, and proliferation, migration, wound healing, and tube formation were suppressed. This result suggested that the high level of *RELB* mRNA could prevent hRECs from undergoing apoptosis in DR.

To study the relationship between *RELB* and miR-1243, OERELB (containing the 5'- and 3'-UTRs) and miR-1243 mimic were co-transfected into hRECs; the miR-1243 mimic conferred the same effects on hRECs as *RELB* knockdown, and the overexpression of *RELB* significantly reversed the effects of miR-1243 mimic. In addition, the overexpression of circ_0008590 could significantly promote the level of *RELB* mRNA and could repress the level of miR-1243. With regard to the physiology of hRECs, high levels of circ_0008590 conferred the same effects as *RELB*, and the effects of miR-1243 mimic were also reversed by the overexpression of circ_0008590. Through the noncanonical pathway, RELB can regulate downstream signaling through interaction with p100, forming the RELB-p52 protein complex; however, in the absence of the 5'- and 3'-ends of circ_0008590, there is no protein product, so it should instead regulate the level of *RELB* mRNA and prevent apoptosis in hRECs by binding directly to miR-1243.

As previously reported, retinal vascular leakage, thickening of the basement membrane, and the loss of retinal pericytes are the most significant clinicopathological features of the progression of DR (37,43,44). The miRNA miR-1243 is unique to human cells; also, owing to the absence of its direct target in the 3'-UTR of mouse *RELB* mRNA, the function of miR-1243 could not be directly determined from the STZ-induced mouse model of DR. In STZ-induced DR mice, abnormal expression levels of circRNAs from *RELB* or some miRNAs may also be induced by hyperglycemia; however, in this work, they were considered to be background changes, and the experiments were designed to investigate the direct interaction between human *RELB* and miR-1243. Human RELB has relatively high similarity and identity with mouse RELB, suggesting that it would play the same role in the progress of DR in mice. Indeed, the overexpression of human or mouse *RELB* did significantly exacerbate the clinicopathological features of DR in mice, whereas the co-injection of miR-1243 agomir partially reversed the effects of the overexpression of human *RELB*.

As previously reported, miR-1243 could also directly bind with hsa_circ_0002570 and angiomotin mRNA, and miR-1243 and hsa_circ_0002570 are mutual inhibitors of each other; moreover, the knockdown of hsa_circ_0002570 inhibited proliferation, migration, tube formation, and the release of pro-inflammatory cytokines induced by hyperglycemia in hRECs (12). In this work, the direct interaction between *RELB* mRNA/circ_0008590 and miR-1243 was confirmed, suggesting that miR-1243 may be a key molecule in hRECs in DR, and that miR-1243 may be part of the self-protection mechanism during the development of DR through its effect on multiple signaling pathways. During the progression of DR, the increase in miR-1243 during the relatively mild stage (NPDR) may be a self-protection phenomenon to repress the transcription of *RELB*; then, as a feedback response in the severe stage (PDR), more circ_0008590 may be produced during the transcription of the *RELB* gene, to suppress miR-1243 and further increase the level of *RELB* mRNA (*Figure 8*).

Conclusions

In this work, the synergistic effect of the interaction between *RELB*/circ_0008590 against miR-1243 in hRECs cultivated in high-glucose conditions was reported for the first time, and the molecular mechanism was investigated *in vivo* and *in vitro*. The results of this study can be considered a reference for the clinical diagnosis and therapy of DR.

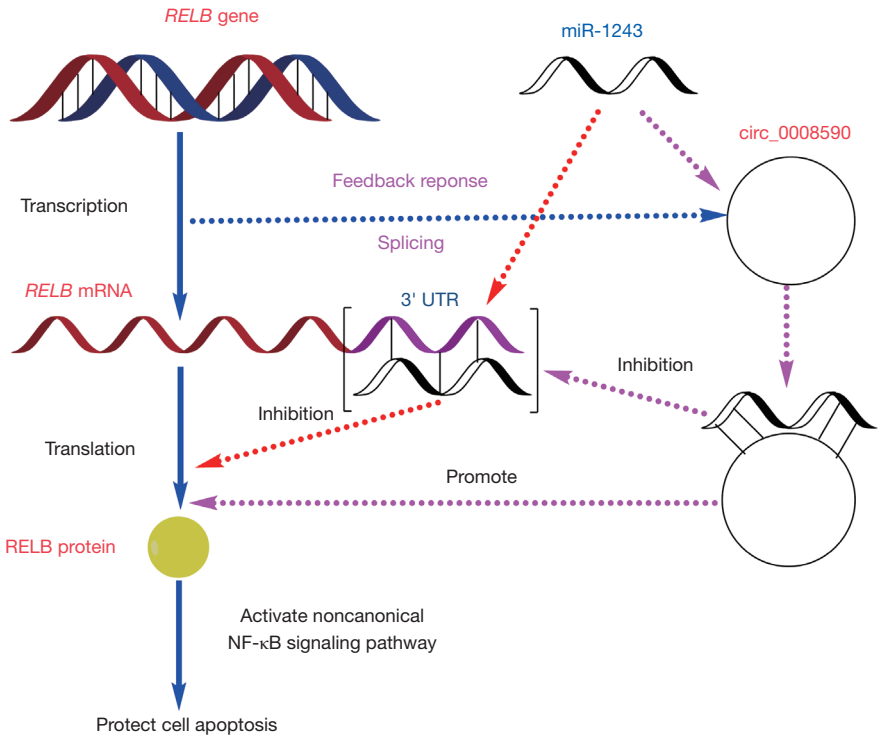

Figure 8 Schematic overview of interaction of *RELB*/circ_0008590 and miR-1243 RELB protected hRECs in hyperglycemia from apoptosis, and miR-1243 promoted the apoptosis ratio by direct binding with the *RELB* mRNA 3'-UTR. In contrast, circ_0008590, a circRNA form of *RELB* was able to recognize miR-1243 using a similar site, subsequently promoting the transcription of RELB, and ultimately preventing apoptosis in hRECs. *RELB*, reticuloendotheliosis viral oncogene related B; hRECs, human retinal microvascular endothelial cells; UTR, untranslated region; circRNA, circular RNA; mRNA, messenger RNA.

Acknowledgments

Funding: This work was supported by National Natural Science Foundation of China (81970819), China Postdoctoral Science Foundation (2020M671541), Youth Medical Talent Project of Jiangsu Province (QNRC2016182), and Top Talent Support Program for Young and Middle-Aged People of Wuxi Health Committee (BJ2020012).

Footnote

Reporting Checklist: The authors have completed the ARRIVE reporting checklist. Available at https://dx.doi.org/10.21037/atm-21-5562

Data Sharing Statement: Available at https://dx.doi.org/10.21037/atm-21-5562

Conflicts of Interest: All authors have completed the ICMJE uniform disclosure form (available at https://dx.doi.org/10.21037/atm-21-5562). The authors have no conflicts of interest to declare.

Ethical Statement: The authors are accountable for all aspects of the work in ensuring that questions related to the accuracy or integrity of any part of the work are appropriately investigated and resolved. The study followed the tenets of the Declaration of Helsinki (as revised in 2013) and the ARVO statement for research involving human subjects and was approved by the Ethics Committee of Nanjing Medical University (2019-398 approved on 25 February 2019). Patients who met the inclusion criteria were informed of the details of the research and signed an informed consent form. All animal experiments adhered to institutional guidelines for humane treatment of animals, the

Principles of Laboratory Animal Care (National Institutes of Health, Bethesda, MD, USA), and the Association for Research in Vision and Ophthalmology (ARVO) Statement for the Use of Animals in Ophthalmic and Vision Research. The animal experiments in this study were approved by the Ethics Committee of Nanjing Medical University (2019-398 approved on 25 February 2019).

References

1. Hammes HP. Diabetic retinopathy: hyperglycaemia, oxidative stress and beyond. Diabetologia 2018;61:29-38.
2. Fickweiler W, Aiello LP, Sun JK, et al. Retinol binding protein 3 as biomarker for diabetic retinopathy. Ann Transl Med 2019;7:706.
3. Solomon SD, Chew E, Duh EJ, et al. Diabetic retinopathy: a position statement by the American Diabetes Association. Diabetes Care 2017;40:412-8. Erratum in: Diabetes Care 2017;40:809. Erratum in: Diabetes Care 2017;40:1285.
4. Thomas RL, Halim S, Gurudas S, et al. IDF Diabetes Atlas: A review of studies utilising retinal photography on the global prevalence of diabetes related retinopathy between 2015 and 2018. Diabetes Res Clin Pract 2019;157:107840.
5. Lu L, Jiang Y, Jaganathan R, et al. Current Advances in Pharmacotherapy and Technology for Diabetic Retinopathy: A Systematic Review. J Ophthalmol 2018;2018:1694187.
6. Gross JG, Glassman AR, Liu D, et al. Five-Year Outcomes of Panretinal Photocoagulation vs Intravitreous Ranibizumab for Proliferative Diabetic Retinopathy: A Randomized Clinical Trial. JAMA Ophthalmol 2018;136:1138-48.
7. Kim JW, Ngai LK, Sadda S, et al. Retcam fluorescein angiography findings in eyes with advanced retinoblastoma. Br J Ophthalmol 2014;98:1666-71.
8. Thomas AS, Hsu ST, House RJ, et al. Microvascular Features of Treated Retinoblastoma Tumors in Children Assessed Using OCTA. Ophthalmic Surg Lasers Imaging Retina 2019;51:43-9.
9. Kim DY, Choi JA, Koh JY, et al. Efficacy and safety of aflibercept in in vitro and in vivo models of retinoblastoma. J Exp Clin Cancer Res 2016;35:171.
10. Wang H, Xiang Y, Hu R, et al. Research progress of circular RNA in digestive tract tumors: a narrative review. Transl Cancer Res 2020;9:7632-41.
11. Ji X, Shan L, Shen P, et al. Circular RNA circ_001621 promotes osteosarcoma cells proliferation and migration by sponging miR-578 and regulating VEGF expression. Cell Death Dis 2020;11:18.
12. Liu G, Zhou S, Li X, et al. Inhibition of hsa_circ_0002570 suppresses high-glucose-induced angiogenesis and inflammation in retinal microvascular endothelial cells through miR-1243/angiomotin axis. Cell Stress Chaperones 2020;25:767-77.
13. Zhang SJ, Chen X, Li CP, et al. Identification and Characterization of Circular RNAs as a New Class of Putative Biomarkers in Diabetes Retinopathy. Invest Ophthalmol Vis Sci 2017;58:6500-9.
14. Zou J, Liu KC, Wang WP, et al. Circular RNA COL1A2 promotes angiogenesis via regulating miR-29b/VEGF axis in diabetic retinopathy. Life Sci 2020;256:117888.
15. Sun H, Kang X. hsa_circ_0041795 contributes to human retinal pigment epithelial cells (ARPE 19) injury induced by high glucose via sponging miR-646 and activating VEGFC. Gene 2020;747:144654.
16. Liu C, Ge HM, Liu BH, et al. Targeting pericyte-endothelial cell crosstalk by circular RNA-cPWWP2A inhibition aggravates diabetes-induced microvascular dysfunction. Proc Natl Acad Sci U S A 2019;116:7455-64.
17. He M, Zhou R, Liu S, et al. Circular RNAs: Potential Star Molecules Involved in Diabetic Retinopathy. Curr Eye Res 2021;46:277-83.
18. Zhang Q, Lenardo MJ, Baltimore D. 30 Years of NF-κB: A Blossoming of Relevance to Human Pathobiology. Cell 2017;168:37-57.
19. Sun SC. The non-canonical NF-κB pathway in immunity and inflammation. Nat Rev Immunol 2017;17:545-58.
20. Knyazev EN, Mal'tseva DV, Zacharyants AA, et al. TNFα-Induced Expression of Transport Protein Genes in HUVEC Cells Is Associated with Enhanced Expression of Transcription Factor Genes RELB and NFKB2 of the Non-Canonical NF-κB Pathway. Bull Exp Biol Med 2018;164:757-61.
21. Cildir G, Low KC, Tergaonkar V. Noncanonical NF-κB Signaling in Health and Disease. Trends Mol Med 2016;22:414-29.

22. Puthanmadhom Narayanan S, Lee JH, Bhagwate A, et al. Epigenetic Alterations Are Associated With Gastric Emptying Disturbances in Diabetes Mellitus. Clin Transl Gastroenterol 2020;11:e00136.
23. Singh MK, Singh L, Chosdol K, et al. Differential expression of p52 and RelB proteins in the metastatic and non-metastatic groups of uveal melanoma with patient outcome. J Cancer Res Clin Oncol 2019;145:2969-82.
24. Zhang S, Patel A, Chu C, et al. Aryl hydrocarbon receptor is necessary to protect fetal human pulmonary microvascular endothelial cells against hyperoxic injury: Mechanistic roles of antioxidant enzymes and RelB. Toxicol Appl Pharmacol 2015;286:92-101.
25. Vallabhapurapu SD, Noothi SK, Pullum DA, et al. Transcriptional repression by the HDAC4-RelB-p52 complex regulates multiple myeloma survival and growth. Nat Commun 2015;6:8428.
26. Xi X, McMillan DH, Lehmann GM, et al. Ocular fibroblast diversity: implications for inflammation and ocular wound healing. Invest Ophthalmol Vis Sci 2011;52:4859-65.
27. Maass PG, Glažar P, Memczak S, et al. A map of human circular RNAs in clinically relevant tissues. J Mol Med (Berl) 2017;95:1179-89.
28. Shao J, Pan X, Yin X, et al. KCNQ1OT1 affects the progression of diabetic retinopathy by regulating miR-1470 and epidermal growth factor receptor. J Cell Physiol 2019;234:17269-79.
29. Shao J, Fan G, Yin X, et al. A novel transthyretin/STAT4/miR-223-3p/FBXW7 signaling pathway affects neovascularization in diabetic retinopathy. Mol Cell Endocrinol 2019;498:110541.
30. Shao J, Zhang Y, Fan G, et al. Transcriptome analysis identified a novel 3-LncRNA regulatory network of transthyretin attenuating glucose induced hRECs dysfunction in diabetic retinopathy. BMC Med Genomics 2019;12:134.
31. Brown J, Pirrung M, McCue LA. FQC Dashboard: integrates FastQC results into a web-based, interactive, and extensible FASTQ quality control tool. Bioinformatics 2017;33:3137-9.
32. Dai M, Thompson RC, Maher C, et al. NGSQC: cross-platform quality analysis pipeline for deep sequencing data. BMC Genomics 2010;11 Suppl 4:S7.
33. Kim D, Pertea G, Trapnell C, et al. TopHat2: accurate alignment of transcriptomes in the presence of insertions, deletions and gene fusions. Genome Biol 2013;14:R36.
34. Jeck WR, Sorrentino JA, Wang K, et al. Circular RNAs are abundant, conserved, and associated with ALU repeats. RNA 2013;19:141-57.
35. Zhang XO, Wang HB, Zhang Y, et al. Complementary sequence-mediated exon circularization. Cell 2014;159:134-47.
36. Fan G, Gu Y, Zhang J, et al. Transthyretin Upregulates Long Non-Coding RNA MEG3 by Affecting PABPC1 in Diabetic Retinopathy. Int J Mol Sci 2019;20:6313.
37. Jiang H, Zhang H, Jiang X, et al. Overexpression of D-amino acid oxidase prevents retinal neurovascular pathologies in diabetic rats. Diabetologia 2021;64:693-706.
38. Shan K, Liu C, Liu BH, et al. Circular Noncoding RNA HIPK3 Mediates Retinal Vascular Dysfunction in Diabetes Mellitus. Circulation 2017;136:1629-42.
39. Hainsworth DP, Katz ML, Sanders DA, et al. Retinal capillary basement membrane thickening in a porcine model of diabetes mellitus. Comp Med 2002;52:523-9.
40. Kim D, Mecham RP, Nguyen NH, et al. Decreased lysyl oxidase level protects against development of retinal vascular lesions in diabetic retinopathy. Exp Eye Res 2019;184:221-6.
41. Mesquida M, Drawnel F, Fauser S. The role of inflammation in diabetic eye disease. Semin Immunopathol 2019;41:427-45.
42. Wang M, Wang Y, Xie T, et al. Prostaglandin E2/EP2 receptor signalling pathway promotes diabetic retinopathy in a rat model of diabetes. Diabetologia 2019;62:335-48.
43. Kur J, Newman EA, Chan-Ling T. Cellular and physiological mechanisms underlying blood flow regulation in the retina and choroid in health and disease. Prog Retin Eye Res 2012;31:377-406.
44. Corliss BA, Ray HC, Doty RW, et al. Pericyte Bridges in Homeostasis and Hyperglycemia. Diabetes 2020;69:1503-17.

(English Language Editor: J. Jones)

Cite this article as: Shao J, Cai J, Yao Y, Zhu H. Hyperglycemia-induced increasing of *RELB*/circ_0008590 in NF-κB pathway is repressed by miR-1243 in human retinal microvascular endothelial cells. Ann Transl Med 2021;9(21):1624. doi: 10.21037/atm-21-5562

